

Zinc Inhibition of Potassium Efflux in Depolarized Frog Muscle and Its Modification by External Hydrogen Ions and Diethylpyrocarbonate Treatment

Bruce C. Spalding, John G. Swift, and Paul Horowicz

Department of Physiology, School of Medicine and Dentistry, University of Rochester, Rochester, New York 14642

Summary. Efflux of $^{42}\text{K}^+$ was measured in frog sartorius muscles equilibrated in hyperosmotic depolarizing solutions. At the internal potentials obtained, K^+ passes mainly through the inward rectifier potassium channels.

Inhibition of K^+ efflux by external Zn^{2+} (0.25 to 15 mM) differs in three significant ways from inhibition by Ba^{2+} . (1) The dose-response relation does not correspond to action at a single site. (2) The Zn^{2+} -sensitivity of K^+ efflux does not depend on $[\text{K}^+]_o$ at constant internal potential. (3) Zn^{2+} inhibition is reduced by hydrogen ions, while Ba^{2+} inhibition is unaffected. Further, the Ba^{2+} -sensitivity of K^+ efflux is not altered by a half-inhibiting Zn^{2+} concentration, suggesting that the two ions do not interact at a common site.

The histidine-modifying reagent diethylpyrocarbonate (DEPC) reduces Zn^{2+} inhibition. After DEPC treatment Zn^{2+} inhibition is further reduced by low pH. DEPC has little effect on Ba^{2+} inhibition. Zn^{2+} inhibition is not altered by treatment with the sulfhydryl reagents 5,5'-dithio-bis(2-nitrobenzoic acid) or dithiothreitol.

The results can be described by either of two models in which two sites can bind Zn^{2+} and one or both of the sites may also bind H^+ . When both sites bind Zn^{2+} , K^+ efflux is inhibited, and a third site may then bind H^+ . The effects of DEPC can be accounted for by a decrease in H^+ affinity of the first two sites by a factor of 50, and a decrease in Zn^{2+} affinity of these sites and of the H^+ affinity of the third site by about one order of magnitude.

Key Words anomalous rectifier · inward rectifier · potassium efflux · zinc · muscle membrane · diethylpyrocarbonate

Introduction

The effects of extracellular Zn^{2+} on frog skeletal muscle differ, depending on the concentration range. External Zn^{2+} up to about 0.1 mM produces twitch potentiation (Isaacson & Sandow, 1963; Sandow, Taylor, Isaacson & Seguin, 1964) and a parallel prolongation of the falling phase of the action potential (Mashima & Washio, 1964; Sandow et al., 1964; Edman & Grieve, 1966) principally caused by a slowing of potassium currents through the delayed rectifier (Stanfield, 1975). There is little change in

the overshoot or maximum rate of rise of the action potential (Mashima & Washio, 1964; Sandow et al., 1964; Sandow & Pagala, 1978).

For $[\text{Zn}^{2+}]_o$ between 0.1 and 1.0 mM, the action potential duration continues to increase (Mashima & Washio, 1964; Taylor, Preiser & Sandow, 1972), the maximum rate of depolarization and overshoot are reduced (Taylor et al., 1972; Sandow & Pagala, 1978), and there is a decrease in membrane chloride conductance with little change in the resting potassium conductance (Mashima & Washio, 1964; Hutter & Warner, 1967b; Stanfield, 1970). The resting membrane potassium conductance in frog skeletal muscle fibers is generally ascribed to the inward potassium rectifier (Katz, 1949; Hodgkin & Horowicz, 1959; Adrian & Freygang, 1962).

In this report it is shown that external Zn^{2+} in concentrations above 1 mM reduces potassium efflux through the inward potassium rectifier in depolarized fibers. The mode of action of Zn^{2+} is shown to differ from that of Ba^{2+} . A preliminary account of these results has been presented (Spalding, Swift & Horowicz, 1984).

Materials and Methods

In these experiments, $^{42}\text{K}^+$ efflux from sartorius muscles from the frog *Rana pipiens* was measured using the procedures described in the preceding paper (Spalding, Swift & Horowicz, 1986). K^+ efflux was calculated as the fraction of radioactive potassium lost from the muscle, expressed as an apparent efflux rate coefficient, k , and referred to simply as “ K^+ efflux” with the units of min^{-1} .

The solutions used in this study are identified by the concentration (in mM) of K^+ and Na^+ (as the chloride salt) used in their preparation, for example “150- K^+ , 120- Na^+ ” solution. In addition, solutions contained 5 mM MgCl_2 and 1 mM CaCl_2 and tris, HEPES, PIPES or MES buffer. Solutions containing zinc or barium are prepared by using ZnCl_2 or BaCl_2 to replace an equimolar concentration of MgCl_2 up to 5 mM, or to replace NaCl at

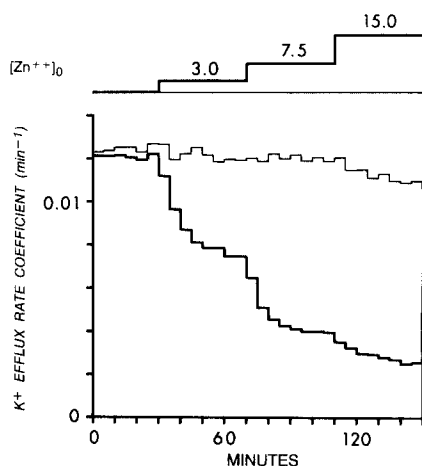


Fig. 1. Reduction in K^+ efflux by Zn^{2+} in muscles bathed in 150- K^+ , 120- Na^+ solution at pH 6.8. K^+ efflux rate coefficients during each collection period in the presence (thick line) or absence (thin line) of the $[Zn^{2+}]_0$ indicated are plotted

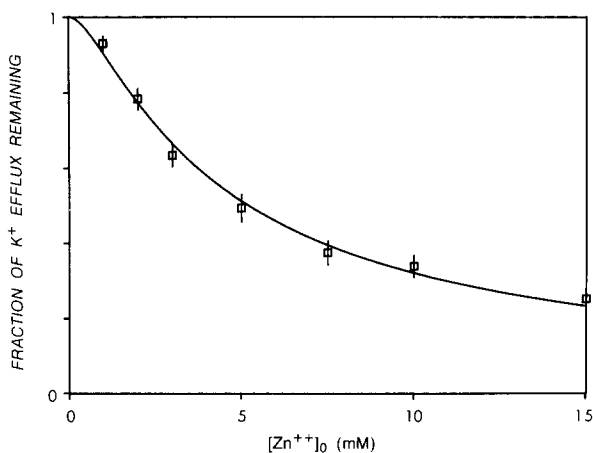


Fig. 2. Zn^{2+} inhibition of K^+ efflux for 17 muscle pairs bathed in 150- K^+ , 120- Na^+ solution at pH 6.8, as in Fig. 1. The points are means from nine experiments of the ratio of the K^+ efflux rate coefficient in the $[Zn^{2+}]_0$ indicated to that in the control muscle in Zn^{2+} -free solution at the same time, normalized to this ratio before exposure to Zn^{2+} . Vertical bars indicate \pm SE. The curve is drawn according to Eq. (1) with $C_0 = 1.1 \times 10^4 \text{ mm}^{-1}$, $C_1 = 1.1 \text{ mm}^{-1}$, $C_2 = 1.2 \times 10^3 \text{ mm}^{-1}$ and $[H^+]_0 = 1.58 \times 10^{-4} \text{ mm}$ (pH = 6.8)

the rate of 3 mM NaCl per 2 mM divalent salt beyond 5 mM. For solutions containing Ba^{2+} and a fixed concentration of Zn^{2+} , the concentration of $MgCl_2$ in the Zn^{2+} -free solutions was increased so that the total divalent concentration was the same as in the Zn^{2+} -containing solutions.

Treatment with diethylpyrocarbonate (DEPC) was performed as follows: to minimize loss of reagent to hydrolysis (Fedorcsák and Ehrenberg, 1966; Shrager, 1974), solid DEPC was dissolved in solution containing maleate buffer at pH 6.0 immediately before it was applied. This solution was then used to fill a series of 5 to 8 collection tubes for each muscle to be

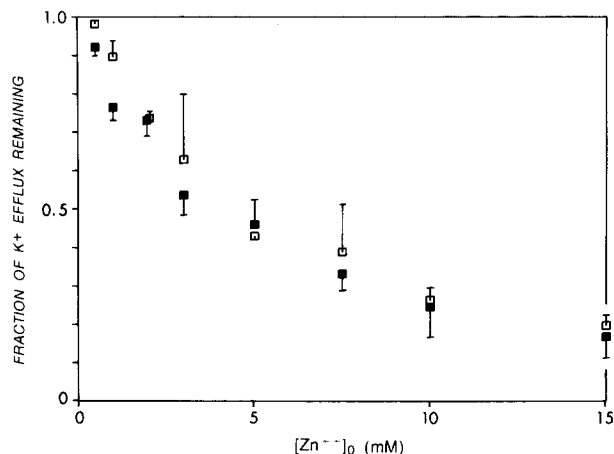


Fig. 3. Comparison of Zn^{2+} inhibition of K^+ efflux for four muscle pairs bathed in 100- K^+ , 60- Na^+ solution at pH 7 ($V_i = -18.1 \text{ mV}$, open symbols) and four muscle pairs bathed in 200- K^+ , 240- Na^+ solution at pH 7.1 ($V_i = -19.8 \text{ mV}$, filled symbols). The points are means of the ratio of the K^+ efflux rate coefficient in the $[Zn^{2+}]_0$ indicated to that in the control muscle in Zn^{2+} -free solution at the same time, normalized to this ratio before exposure to Zn^{2+} . The bars indicate standard deviations from two determinations. For clarity, overlapping symbols have been offset slightly along the abscissa

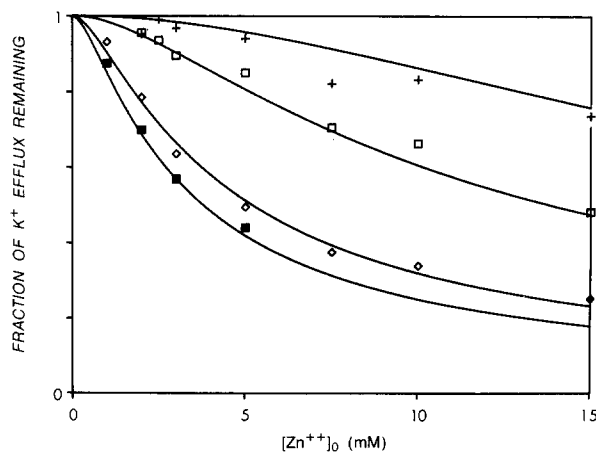


Fig. 4. Comparison of Zn^{2+} inhibition of K^+ efflux for muscles bathed in 150- K^+ , 120- Na^+ solution at pH 7.11 (two muscle pairs, ■), 6.8 (17 muscle pairs, ◇), 6.0 (four muscle pairs, □) and 5.2 (seven muscle pairs, +). The points are the ratio of the K^+ efflux rate coefficient in the $[Zn^{2+}]_0$ indicated to that in the control muscle in Zn^{2+} -free solution at the same time, normalized to this ratio before exposure to Zn^{2+} . The curves are drawn according to Eq. (1) with C_0 , C_1 , and C_2 as in Fig. 2 and $[H^+]_0$ appropriate for pH 7.11, 6.8, 6.0 and 5.2

treated, so that collection of $^{42}K^+$ leaving the cell was not interrupted by DEPC treatment. DEPC was applied at concentrations of 0.75 mM for 25 min or 1.5 mM for 30 or 40 min; DEPC appeared to be equally effective at all of the concentrations and treatment times used.

Table. K⁺ efflux rate coefficients at various pH values

Solution	pH	k ($\times 10^{-3} \text{ min}^{-1}$)	n	$k/k(\text{pH } 7.2)$
150,120	7.2	16.14 ± 0.31	76	
150,120	6.8	15.32 ± 0.43	144	0.95
150,120	6.0	15.51 ± 0.33	24	0.96
150,120	5.2	17.67 ± 0.70	28	1.09

Results

Millimolar external Zn²⁺ reduces potassium efflux through the inward rectifier potassium channel. The K⁺ efflux in 150-K⁺, 120-Na⁺ solution at three external Zn²⁺ concentrations is shown in Fig. 1. Although the concentration dependence of Zn²⁺ inhibition is similar to that of Ba²⁺ (Spalding et al., 1986), the Zn²⁺ effect takes longer to reach a steady level.

The concentration dependence of the mean K⁺ efflux remaining in a given [Zn²⁺]_o shown in Fig. 2 does not correspond to binding of Zn²⁺ to a single site, as will be seen more clearly later. Instead, we describe the Zn²⁺ effect by a model which leads to the equation:

$$u = \frac{1}{1 + \frac{(1 + C_1[H^+]_o)(C_1[Zn^{2+}]_o)^2}{(1 + C_0[H^+]_o)(1 + C_0[H^+]_o + 2C_1[Zn^{2+}]_o)}} \quad (1)$$

where u is the fraction of K⁺ efflux remaining in the presence of Zn²⁺, as plotted in Fig. 2. The curve in Fig. 2 is drawn according to Eq. (1) with $C_0 = 1.1 \times 10^4 \text{ mM}^{-1}$; $[H^+]_o = 1.58 \times 10^{-4} \text{ mM}$ (pH = 6.8); $C_1 = 1.1 \text{ mM}^{-1}$; and $C_2 = 1.2 \times 10^3 \text{ mM}^{-1}$.

In the previous paper (Spalding et al., 1986), the reduction of K⁺ efflux by Ba²⁺ was described by

$$u = (u_1/(1 + C[Ba^{2+}]_o)) + u_2 \quad (2)$$

where $u_1 + u_2 = 1$. The form of the equation is not the same and reflects a significant difference between the effects of the two ions.

Inhibition by Zn²⁺ also differs from that by Ba²⁺ in being insensitive to external potassium. Figure 3 compares Zn²⁺ inhibition of K⁺ efflux in two solutions with different potassium concentrations (100 and 200 mM) but approximately the same resting potential (-18.1 and -19.8 mV, respectively; see Table 1 of Spalding et al., 1986). There is no significant difference in the fractional reduction of K⁺ efflux by Zn²⁺ between the two solutions. In contrast Ba²⁺ sensitivity is over three times higher in 100-K⁺ than in 200-K⁺ (Spalding et al., 1986).

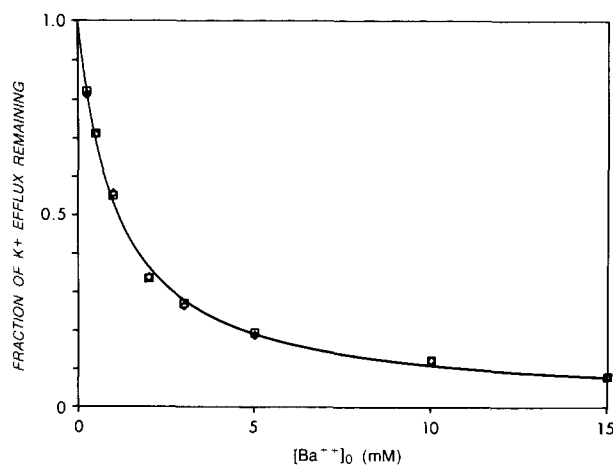


Fig. 5. Comparison of Ba²⁺ inhibition of K⁺ efflux for four muscle pairs bathed in 150-K⁺, 120-Na⁺ solution at pH 7.3 (□) and four muscle pairs bathed in 150-K⁺, 120-Na⁺ solution at pH 5.2 (◇). The points are means of the ratio of the K⁺ efflux rate coefficient in the [Ba²⁺]_o indicated to that in the control muscle in Ba²⁺-free solution at the same time, normalized to this ratio before exposure to Ba²⁺. The curves are drawn according to Eq. (2) with $C = 0.89$ and 0.89 mM^{-1} and $u_2 = 0.0096$ and 0.0075 at pH 7.3 and 5.2, respectively

Zn²⁺ inhibition is reduced by increases in external hydrogen ion concentration, as shown in Fig. 4. The curves, drawn according to Eq. (1) with the values of C_0 , C_1 and C_2 as in Fig. 2, adequately describe the effects of H⁺ on Zn²⁺ inhibition. As shown in the Table, K⁺ efflux in the absence of Zn²⁺ is little affected by external pH, in agreement with earlier reports that the inward rectifier is not sensitive to external pH (Hutter & Warner, 1967a; Blatz, 1984).

The pH sensitivity of the Zn²⁺ effect, like the insensitivity to K⁺, distinguishes the effects of Zn²⁺ from those of Ba²⁺. Figure 5 shows that pH changes from pH 5.2 to 7.3 have no effect on Ba²⁺ inhibition.

To summarize, changes in [K⁺]_o alter the sensitivity of K⁺ efflux to Ba²⁺ but not to Zn²⁺, and changes in pH alter the sensitivity to Zn²⁺ but not to Ba²⁺. Evidently, the two divalent ions act at distinct sites.

This has been further examined by comparing the reduction in K⁺ efflux by Ba²⁺ in the presence and absence of an approximately half-saturating concentration (5 mM) of Zn²⁺. Figure 6 shows the Ba²⁺ sensitivity of K⁺ efflux in the presence and absence of 5 mM Zn²⁺. (The total divalent ion concentration was the same in all solutions; see Materials and Methods.) The Ba²⁺ sensitivity is little changed by Zn²⁺, consistent with independent sites of action. Similar results were obtained in other experiments using 1 mM Zn²⁺, involving eight muscle pairs. The main difference between the two curves

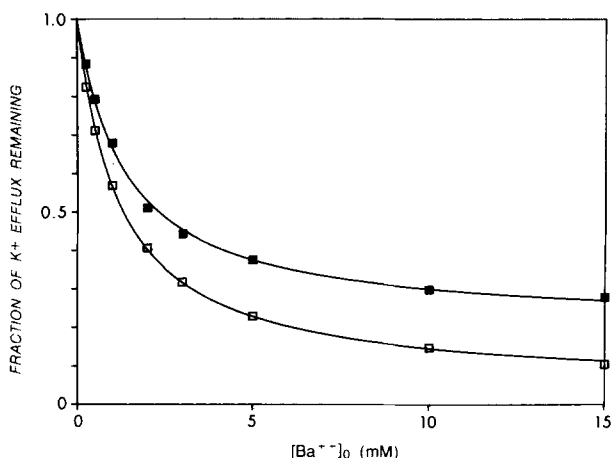


Fig. 6. Comparison of Ba^{2+} inhibition of K^+ efflux muscle pairs bathed in 150- K^+ , 120- Na^+ solution at pH 6.8 in the presence (eight pairs, ■) or absence (eight pairs, □) of 5 mM Zn^{2+} . The points are means of the ratio of the K^+ efflux rate coefficient in the $[Ba^{2+}]_o$ indicated to that in the control muscle in Ba^{2+} -free solution at the same time, normalized to this ratio before exposure to Ba^{2+} . The curves are drawn according to Eq. (2) with $C = 0.73$ and 0.84 mM^{-1} and $u_2 = 0.20$ and 0.04 in the presence and absence of Zn^{2+} , respectively

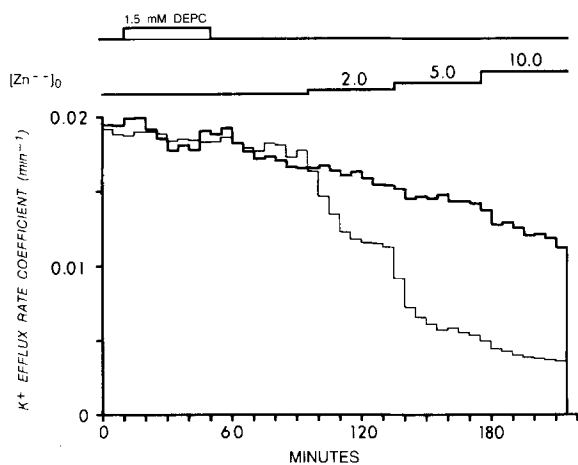


Fig. 7. Effect of diethylpyrocarbonate on the reduction in K^+ efflux by Zn^{2+} . K^+ efflux rate coefficients during each collection period in a muscle treated for 40 min with 1.5 mM diethylpyrocarbonate (thick line) at pH = 6.0 and an untreated muscle (thin line) bathed in 150- K^+ , 120- Na^+ solution at pH 6.8 with the $[Zn^{2+}]_o$ indicated were plotted. For both the treated and untreated muscle $[Zn^{2+}]_o$ was increased as indicated. The efflux experiments on the two muscles were performed concurrently, but the muscles were not from the same frog

in Fig. 6 is that the Ba^{2+} -resistant K^+ efflux makes up a larger fraction of the smaller total efflux in the Zn^{2+} -containing solution. For the experiments of Fig. 6, when $[Ba^{2+}]_o = 0$, the mean K^+ efflux rate coefficient in 5- Zn^{2+} solution is 0.50 that in the Zn^{2+} -free solution, while when $[Ba^{2+}]_o = 10$ or 15 mM, the mean rate coefficients in 5- Zn^{2+} solution

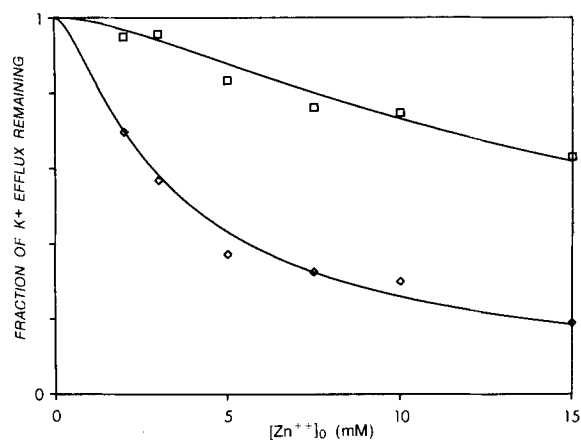


Fig. 8. Zn^{2+} inhibition of K^+ efflux for four muscle pairs after treatment with diethylpyrocarbonate (□) and four untreated muscle pairs (◇). Muscles were bathed in 150- K^+ , 120- Na^+ solution at pH 6.8, as in Fig. 7. The points are the ratio of the K^+ efflux rate coefficient in the $[Zn^{2+}]_o$ indicated to that in the control muscle in Zn^{2+} -free solution at the same time, normalized to this ratio before exposure to Zn^{2+} . The curves are drawn according to Eq. (1) with $C_0 = 200 \text{ mM}^{-1}$, $C_1 = 0.11 \text{ mM}^{-1}$ and $C_2 = 100 \text{ mM}^{-1}$ for the treated muscles and $C_0 = 10^4 \text{ mM}^{-1}$, $C_1 = 1.4 \text{ mM}^{-1}$ and $C_2 = 10^3 \text{ mM}^{-1}$ for the untreated muscles

are not significantly different from those in Zn^{2+} -free solution (two-tailed t test). The larger u_2 in 5- Zn^{2+} solution is partially explained by this difference alone. Further, these results suggest that the Ba^{2+} -resistant K^+ efflux is not reduced by 5 mM Zn^{2+} .

The pH dependence of Zn^{2+} inhibition suggests that a titratable group with a pK_a between 6 and 7, similar to that of a histidine group, may be involved. We have examined the effects of treating muscles with diethylpyrocarbonate (DEPC) at pH 6, which according to Mùhlrad, Hegyi and Tóth (1967), Mùhlrad, Hegyi and Horányi (1969), and Ovádi, Libor and Elödi (1967), specifically carbethoxylates histidyl residues in proteins. Figure 7 illustrates that treatment with DEPC reduces sensitivity to Zn^{2+} . Figure 8 shows the effect of DEPC treatment on the concentration dependence of Zn^{2+} inhibition. The curves are drawn according to Eq. (1), each with pH = 6.8, but with different values of C_0 and C_1 . The effects of DEPC treatment can be modeled by decreasing C_0 by a factor of 50, corresponding to a shift of 1.7 pH units, and also decreasing C_1 by a factor of 12.7 and C_2 by a factor of 10.

In contrast, Fig. 9 shows that DEPC treatment provides little protection from inhibition by Ba^{2+} . The only effects of DEPC are a small increase in the Ba^{2+} -resistant fraction and a reduction in Ba^{2+} -sensitivity by a factor of about 1.7. It is shown later that lowering the external pH also reduces Zn^{2+} inhibition after DEPC treatment (see Fig. 12).

Treatment with DEPC seems not to affect the

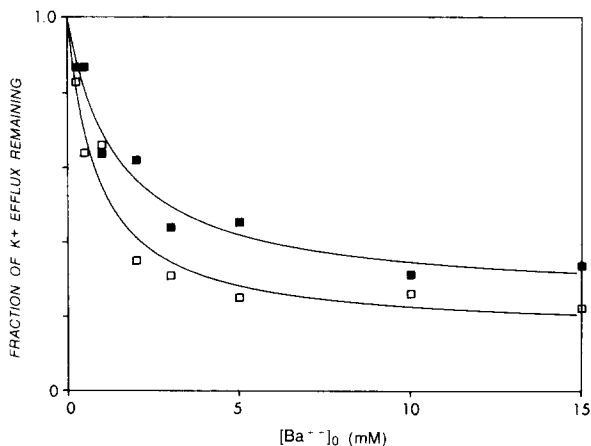


Fig. 9. Ba²⁺ inhibition of K⁺ efflux for muscle pairs treated for 40 min with 1.5 mM diethylpyrocarbonate (filled symbols) and untreated muscle pairs (open symbols). Muscles were bathed in 150-K⁺, 120-Na⁺ solution at pH 6.8. The points are the ratio of the K⁺ efflux rate coefficient in the [Ba²⁺]_o indicated to that in the control muscle in Ba²⁺-free solution at the same time, normalized to this ratio before exposure to Ba²⁺. The curves are drawn according to Eq. (2) with $C = 0.69$ and 1.17 mM^{-1} and $u_2 = 0.25$ and 0.16 for the treated and untreated muscles, respectively

magnitude of K⁺ efflux itself. Efflux rate coefficients after DEPC treatment were not significantly different from those in the control muscles at the same time (mean treated/control of 0.98 ± 0.15 , $n = 16$).

In two experiments involving eight muscle pairs, no significant change in the magnitude of the reduction in K⁺ efflux by [Zn²⁺]_o was observed following treatment with either of the sulfhydryl reagents 5,5'-dithio-bis(2-nitrobenzoic acid) or dithiothreitol (each reagent was applied at 1 mM for 30 min at pH 8.3). Apparently, the pH sensitivity of the Zn²⁺ effect does not involve a titratable sulfhydryl group, or such a group is not accessible to the particular reagents used.

Discussion

A model for Zn²⁺ inhibition should explain both protection by external H⁺ and the shape of the Zn²⁺ inhibition curve at each [H⁺]_o value. In addition, the model should be consistent with the absence of a measurable effect of protonation or carbethoxylation on K⁺ efflux in high external K⁺ solutions. That the steepest part of the *u vs.* [Zn²⁺]_o curve extrapolates to $u = 1$ at [Zn²⁺]_o > 0 indicates more than one site interacts with Zn²⁺. We assume two sites are involved. Protection against Zn²⁺ inhibition by H⁺ occurs between pH 7.0 and 6.0, and since diethylpyrocarbonate treatment also reduces Zn²⁺-sensitivity it is likely that the sites involved

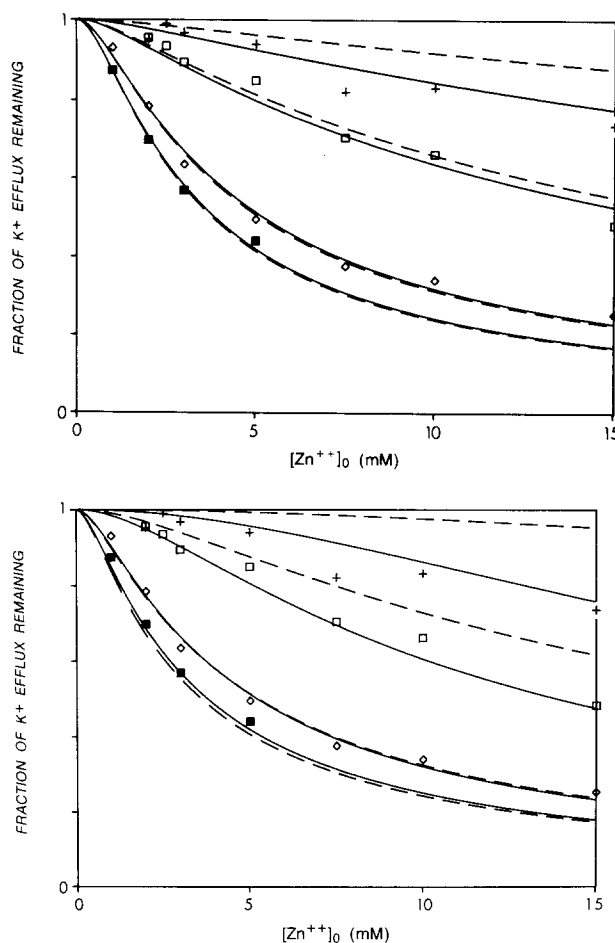


Fig. 10. Fit of models to Zn²⁺ inhibition data at pH 7.11, 6.8, 6.0, and 5.2 from Fig. 4. *Top:* Solid lines are drawn according to Model A, with $C_0 = 1.1 \times 10^4 \text{ mM}^{-1}$, $C_1 = 0.66 \text{ mM}^{-1}$ and $C_2 = 200 \text{ mM}^{-1}$ [see Eq. (A14)]. Dashed lines are drawn according to Model A without stabilization step: $C_0 = 10^4 \text{ mM}^{-1}$, $C_1 = 0.66 \text{ mM}^{-1}$ and $C_2 = 0$. *Bottom:* Solid lines are drawn according to Model B with $C_0 = 1.1 \times 10^4 \text{ mM}^{-1}$, $C_1 = 1.1 \text{ mM}^{-1}$ and $C_2 = 1.2 \times 10^3 \text{ mM}^{-1}$ [see Eq. (1)]. Dashed lines are drawn according to Model B without stabilization step: $C_0 = 10^4 \text{ mM}^{-1}$, $C_1 = 1.2 \text{ mM}^{-1}$ and $C_2 = 0$

are titratable histidine groups associated with the inward rectifier channels.

The additional assumptions are that both sites have the same affinities for H⁺ and Zn²⁺, and that the probability of K⁺ exit is zero when Zn²⁺ is bound to both sites, and unchanged otherwise. Two different models employing the above assumptions can be fit to the Zn²⁺ inhibition results for the pH range between 7.1 and 6.8, but both models then predict less Zn²⁺ inhibition at the more acid pH's than is measured experimentally. Postulating an additional site which can be protonated when the first two sites both bind Zn²⁺ serves to stabilize the Zn²⁺ binding to the first two sites and produces a much better fit to the data for the entire external pH range explored.

These points are illustrated in Fig. 10. The two

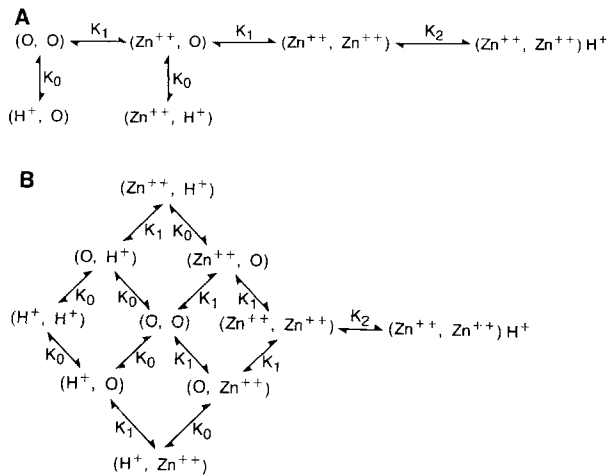


Fig. 11. State diagram for the models described in the text. The symbol for each state indicates the occupancy of the two sites by Zn^{2+} or H^+ . An empty site is denoted by O . The equilibrium constants associated with each reaction under the assumptions of the model are indicated. In the state on the right of each diagram H^+ is bound by a third group made available by the binding of Zn^{2+} by both sites. (A) Model A. (B) Model B

panels show the fit of the two models to the data of Fig. 4. The two models are described in the Appendix, and the state diagrams are shown in Fig. 11. The major difference between the two models is that in Model A, Zn^{2+} gets bound to one site before the second site can bind Zn^{2+} or H^+ , while in Model B, the two Zn^{2+} -binding sites interact with Zn^{2+} and H^+ independently. The dashed lines of Fig. 10 show that when curves are fit to the results at pH 7.1 and 6.8 without the third site, the predicted inhibition in acid pH's underestimates the measured inhibition. The solid lines show that when the stabilization step is included both models yield better fits to the results at all pH's. Reasonably good fits for both models can be obtained with a pK_a of 7.04 for protonation of the Zn^{2+} -binding sites. The Zn^{2+} affinities of the binding sites are greater by two thirds for Model A as compared to Model B. For the third site, the optimum pK_a is 6.08 for Model B and 5.30 for Model A.

Figure 12 shows fits of the models to the pH dependence of Zn^{2+} inhibition after DEPC treatment. The symbols show the relative K^+ efflux at pH 6.8 from DEPC-treated muscles, and from untreated control muscles measured concurrently, and also the relative K^+ efflux at pH 5.2 from additional DEPC-treated muscles. Good fits to the data for both models were obtained with a shift in the pK_a for the protonation of the Zn^{2+} -binding sites of 1.7 pH units. This is somewhat less than the 2-pH unit shift in the pK_a for the imidazole group of histidine after carboxymethylation reported by Mùhlrad et

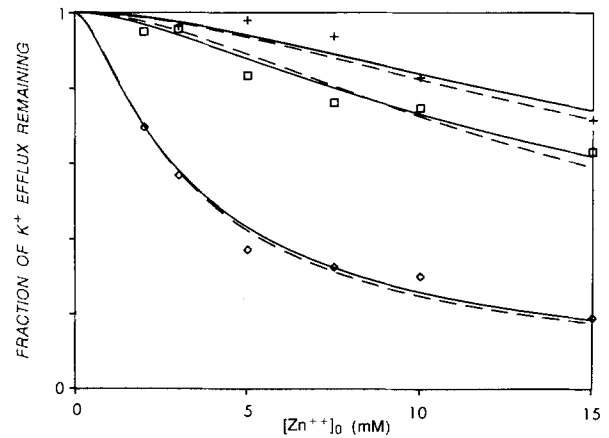


Fig. 12. Fit of models to Zn^{2+} -inhibition data with and without DEPC treatment from Fig. 8 and to Zn^{2+} -inhibition data at pH 5.2 from two additional muscle pairs treated with DEPC (+). Solid lines are drawn according to Model B as in Fig. 8. Dashed lines are drawn according to Model A with $C_0 = 200 \text{ mM}^{-1}$, $C_1 = 0.085 \text{ mM}^{-1}$ and $C_2 = 40 \text{ mM}^{-1}$ for the treated muscles and $C_0 = 10^4 \text{ mM}^{-1}$, $C_1 = 0.85 \text{ mM}^{-1}$ and $C_2 = 200 \text{ mM}^{-1}$ for the untreated muscles

al. (1967). For Model A after DEPC treatment, good fits are obtained by reducing C_1 by a factor of 10 and C_2 by a factor of 5 as compared to the untreated controls. For Model B after DEPC treatment, C_1 is reduced by a factor of 12.7 and C_2 is reduced by a factor of 10. It is clear from Fig. 12 that both models can be made to fit the Zn^{2+} -inhibition data after treatment with DEPC by decreasing the apparent H^+ and Zn^{2+} affinities of the Zn^{2+} -binding sites and the apparent H^+ affinity for the stabilization step by similar factors for the two models.

We conclude that although Ba^{2+} and Zn^{2+} reduce K^+ efflux at similar concentrations, they act by different mechanisms. Lowering the pH interferes with the Zn^{2+} effect, evidently mediated through two titratable histidine groups associated with each inward rectifier channel. The Zn^{2+} effect is insensitive to changes in $[K^+]_o$. Ba^{2+} inhibition, on the other hand, depends on the external K^+ concentration, but is insensitive to pH and only slightly affected by carboxymethylation of histidine groups.

This work was supported by grants from the National Institutes of Health and the Muscular Dystrophy Association. We also wish to thank Dan Gefell and Greg Connors for assistance in some experiments.

References

- Adrian, R.H., Freygang, W.H. 1962. Potassium conductance of frog muscle membrane under controlled voltage. *J. Physiol. (London)* **163**:104-114

- Blatz, A.L. 1984. Asymmetric proton block of inward rectifier K channels in skeletal muscle. *Pfluegers Arch.* **401**:402–407
- Edman, K.A.P., Grieve, D.W. 1966. The relation between the electrical and mechanical activities of single muscle fibres in the presence of zinc. *J. Physiol. (London)* **185**:29–31P
- Fedorcsák, I., Ehrenberg, L. 1966. Effects of diethylpyrocarbonate and methyl methanesulfonate on nucleic acids and nucleases. *Acta Chem. Scand.* **20**:107–112
- Hodgkin, A.L., Horowicz, P. 1959. The influence of potassium and chloride ions on the membrane potential of single muscle fibres. *J. Physiol. (London)* **148**:127–160
- Hutter, O.F., Warner, A.E. 1967a. The pH sensitivity of the chloride conductance of frog skeletal muscle. *J. Physiol. (London)* **189**:403–425
- Hutter, O.F., Warner, A.E. 1967b. Action of some foreign cations and anions on the chloride permeability of frog muscle. *J. Physiol. (London)* **189**:445–460
- Isaacson, A., Sandow, A. 1963. Effects of zinc on responses of skeletal muscle. *J. Gen. Physiol.* **46**:655–677
- Katz, B. 1949. Les constantes électriques de la membrane du muscle. *Arch. Sci. Physiol.* **3**:285–300
- Mashima, H., Washio, H. 1964. The effect of zinc on the electrical properties of membrane and the twitch tension in frog muscle fibres. *Jpn. J. Physiol.* **14**:538–550
- Mühlrad, A., Hegyi, G., Horányi, M. 1969. Studies on the properties of chemically modified actin: III. Carbethoxylation. *Biochim. Biophys. Acta* **181**:184–190
- Mühlrad, A., Hegyi, G., Tóth, G. 1967. Effect of diethylpyrocarbonate on proteins: I. Reaction of diethylpyrocarbonate with amino acids. *Acta Biochim. Biophys. Acad. Sci. Hung.* **2**:19–29
- Ovádi, J., Libor, S., Elödi, P. 1967. Spectrophotometric determination of histidine in proteins with diethylpyrocarbonate. *Acta Biochim. Biophys. Acad. Sci. Hung.* **2**:455–458
- Sandow, A., Pagala, M.K.D. 1978. Detubulation effects on the action of zinc on frog skeletal muscle action potential. *J. Membrane Biol.* **41**:309–321
- Sandow, A., Taylor, S.R., Isaacson, A., Seguin, J.J. 1964. Electrochemical coupling in potentiation of muscular contraction. *Science* **143**:577–579
- Shrager, P. 1974. Ionic conductance changes in voltage clamped crayfish axons at low pH. *J. Gen. Physiol.* **64**:666–690
- Spalding, B.C., Swift, J.G., Horowicz, P. 1984. Zinc and barium inhibition of potassium efflux through the inward rectifier in frog skeletal muscle. *Biophys. J.* **45**:143a
- Spalding, B.C., Swift, J.G., Horowicz, P. 1986. Influence of external barium and potassium on potassium efflux in depolarized frog sartorius muscles. *J. Membrane Biol.* **93**:141–156
- Stanfield, P.R. 1970. The differential effects of tetraethylammonium and zinc ions on the resting conductance of frog skeletal muscle. *J. Physiol. (London)* **209**:231–256
- Stanfield, P.R. 1975. The effect of zinc ions on the gating of the delayed potassium conductance of frog sartorius muscle. *J. Physiol. (London)* **251**:711–735
- Taylor, S.R., Preiser, H., Sandow, A. 1972. Action potential parameters affecting excitation-contraction coupling. *J. Gen. Physiol.* **59**:421–436

Received 10 February 1986; revised 24 June 1986

Appendix

This appendix presents two models of the actions of external Zn²⁺ and external H⁺ on K⁺ efflux through the inward rectifier channels. The following assumptions are made: two sites, associated with each channel, can bind Zn²⁺ or H⁺. The affinities for Zn²⁺ and for H⁺ are the same for both sites. K⁺ efflux is unaltered unless both sites bind Zn²⁺ in which case it becomes negligible. When both sites bind Zn²⁺, an additional group associated with the channel can interact with H⁺.

Model A

The reaction network for the first model is shown in Fig. 11A. An empty site is denoted by *O*. The reaction network is taken to be always at equilibrium. In this model, the two sites bind external Zn²⁺ sequentially. The second site can bind external Zn²⁺ or H⁺ when the first site binds Zn²⁺ but not H⁺. Finally, a third group may bind H⁺ when the two Zn²⁺-binding sites have both bound Zn²⁺. Assuming that the number of channels remains constant,

$$[O,O] + [H^+,O] + [Zn^{2+},O] + [Zn^{2+},H^+] + [Zn^{2+},Zn^{2+}] + [Zn^{2+},Zn^{2+},H^+] = T. \quad (A1)$$

At equilibrium,

$$[H^+,O] = K_0[H^+][O,O] \quad (A2)$$

$$[Zn^{2+},O] = K_1[Zn^{2+}][O,O] \quad (A3)$$

$$[Zn^{2+},H^+] = K_0[H^+][Zn^{2+},O] = K_0K_1[H^+][Zn^{2+}][O,O] \quad (A4)$$

$$[Zn^{2+},Zn^{2+}] = K_1[Zn^{2+}][Zn^{2+},O] = K_1^2[Zn^{2+}]^2[O,O] \quad (A5)$$

$$[Zn^{2+},Zn^{2+},H^+] = K_2[H^+][Zn^{2+},Zn^{2+}] = K_2[H^+](K_1[Zn^{2+}])^2[O,O] \quad (A6)$$

where K_0 , K_1 and K_2 are the equilibrium constants for the individual reactions. Substituting Eqs. (A2) through (A6) into (A1), one obtains

$$[O,O] \cdot Q = T \quad (A7)$$

where

$$Q = (1 + K_0[H^+])(1 + K_1[Zn^{2+}]) + (1 + K_2[H^+])(K_1[Zn^{2+}])^2. \quad (A8)$$

The fraction of channels in any one of the six states is given by the relations:

$$\begin{aligned} f_{OO} &= [O,O]/T; f_{HO} = [H^+,O]/T; f_{ZO} = [Zn^{2+},O]/T; \\ f_{ZZ} &= [Zn^{2+},Zn^{2+}]/T; f_{ZH} = [Zn^{2+},H^+]/T; \\ f_{ZZH} &= [Zn^{2+},Zn^{2+},H^+]/T. \end{aligned} \quad (A9)$$

If the probability of K⁺ exit is zero when both Zn²⁺-binding sites bind Zn²⁺, and is p for all other states, then the total probability of K⁺ exit, k , is

$$k = (f_{00} + f_{H0} + f_{Z0} + f_{ZH})pT. \quad (\text{A10})$$

The uninhibited fraction of K⁺ efflux, after the addition of external Zn²⁺, u , is then

$$u = (f_{00} + f_{H0} + f_{Z0} + f_{ZH}) \quad (\text{A11})$$

since $(f_{00} + f_{H0}) = 1$, $f_{Z0} = 0 = f_{ZH}$, and $k_0 = pT$ when $[\text{Zn}^{2+}]_o = 0$. Substituting Eqs. (A2) through (A9) into (A11) one gets

$$u = \frac{(1 + K_0[\text{H}^+])(1 + K_1[\text{Zn}^{2+}])}{(1 + K_0[\text{H}^+])(1 + K_1[\text{Zn}^{2+}]) + (1 + K_2[\text{H}^+])(K_1[\text{Zn}^{2+}])^2}. \quad (\text{A12})$$

Alternatively, one can write Eq. (A12) as

$$u = \frac{1}{1 + \left[\frac{(1 + K_2[\text{H}^+])(K_1[\text{Zn}^{2+}])^2}{(1 + K_0[\text{H}^+])(1 + K_1[\text{Zn}^{2+}])} \right]}. \quad (\text{A13})$$

For fitting (Figs. 10 and 12), the fitted parameters are labeled C_0 , C_1 and C_2 , where $C_0 = K_0$, $C_1 = K_1$, and $C_2 = K_2$.

Model B

The reaction network for the second model is shown in Fig. 11B. In this model, both sites react with Zn²⁺ and H⁺ independently. An additional state represents, as in Model A, the protonation of a third group when both Zn²⁺-binding sites are occupied by Zn²⁺. Channels are closed for the states denoted by (Zn²⁺, Zn²⁺) and (Zn²⁺, Zn²⁺)H⁺ and open for all other states. Following the same line of development as above for Model A, one obtains the following relation for the uninhibited fraction of K⁺ efflux in the presence of external Zn²⁺:

$$u = \frac{1}{1 + \left[\frac{(K_1[\text{Zn}^{2+}])^2(1 + K_2[\text{H}^+])}{(1 + K_0[\text{H}^+]) + 2K_1[\text{Zn}^{2+}]} \right]}. \quad (\text{A14})$$

Equation (A14) is identical to Eq. (1), with $C_0 = K_0$, $C_1 = K_1$, and $C_2 = K_2$.